

AD-A119 647

CORNELL UNIV ITHACA NY DEPT OF CHEMISTRY

F/6 7/4

SECONDARY ION MASS SPECTROMETRIC IMAGE DEPTH PROFILE ANALYSIS 0--ETC(U)

SEP 82 G H MORRISON, P K CHU, W C HARRIS

N00014-80-C-0538

UNCLASSIFIED

TR-9

NL

| OF |
ADA
-19 647

NOV 1982

END
DATE
FILMED
10 82
DTIC

AD A119647

12

OFFICE OF NAVAL RESEARCH

Contract N00014-80-C-0538

Task No. NR 051-736

TECHNICAL REPORT No. 9

Secondary Ion Mass Spectrometric Image
Depth Profile Analysis of Thin Layers

by

G. H. Morrison, P. K. Chu, W. C. Harris, Jr.

Prepared for Publication

in

Analytical Chemistry

Cornell University
Department of Chemistry
Ithaca, New York 14853

DTIC
ELECTE
SEP 28 1982
H

September 22, 1982

Reproduction in whole or in part is permitted for any purpose
of the United States Government

This document has been approved for public release and sale;
its distribution is unlimited

THE COPY

REPORT DOCUMENTATION PAGE		READ INSTRUCTIONS BEFORE COMPLETING FORM
1. REPORT NUMBER Technical Report No. 9	2. GOVT ACCESSION NO. ADA119647	3. RECIPIENT'S CATALOG NUMBER
4. TITLE (and Subtitle) SECONDARY ION MASS SPECTROMETRIC IMAGE DEPTH PROFILE ANALYSIS OF THIN LAYERS		5. TYPE OF REPORT & PERIOD COVERED Interim Technical Report
		6. PERFORMING ORG. REPORT NUMBER
7. AUTHOR(s) G. H. Morrison, P. K. Chu, and W. C. Harris, Jr.		8. CONTRACT OR GRANT NUMBER(s) N00014-80-C-0538
9. PERFORMING ORGANIZATION NAME AND ADDRESS Department of Chemistry Cornell University, Ithaca, N. Y. 14853		10. PROGRAM ELEMENT, PROJECT, TASK AREA & WORK UNIT NUMBERS NR051-736
11. CONTROLLING OFFICE NAME AND ADDRESS ONR 800 N. Quincy St., Arlington, VA 22217		12. REPORT DATE September 22, 1982
		13. NUMBER OF PAGES 20
14. MONITORING AGENCY NAME & ADDRESS (if different from Controlling Office)		15. SECURITY CLASS. (of this report) Unclassified
		15a. DECLASSIFICATION/DOWNGRADING SCHEDULE
16. DISTRIBUTION STATEMENT (of this Report) Approved for public release: distribution unlimited		
17. DISTRIBUTION STATEMENT (of the abstract entered in Block 20, if different from Report)		
18. SUPPLEMENTARY NOTES Prepared for publication in ANALYTICAL CHEMISTRY		
19. KEY WORDS (Continue on reverse side if necessary and identify by block number) Secondary Ion Mass Spectrometry (SIMS), Image Depth Profiling, Thin layer analysis, Ion Implantation, Molecular Beam Epitaxy (MBE), Diffusion.		
20. ABSTRACT (Continue on reverse side if necessary and identify by block number) Image depth profiling is applied to the quantitative analysis of molecular beam epitaxially grown gallium arsenide thin layers. The technique involves the use of ion implantation through a mask and subsequent analysis by secondary ion mass spectrometry (SIMS). The proposed approach provides high accuracy results in the analysis of semiconductor thin layers.		

SECONDARY ION MASS SPECTROMETRIC IMAGE DEPTH PROFILE ANALYSIS OF THIN LAYERS

Paul K. Chu, William C. Harris, Jr., and George H. Morrison *
 Baker Laboratory
 Department of Chemistry
 Cornell University
 Ithaca, New York 14853

BRIEF: The technique of secondary ion mass spectrometric image depth profiling is used to measure the dopant concentration in thin layers of semiconductor materials with the use of masked ion implantation.



Accession For	
NTIS GRA&I	<input checked="" type="checkbox"/>
DTIC TAB	<input type="checkbox"/>
Unannounced	<input type="checkbox"/>
Justification	
By	
Distribution/	
Availability Codes	
Dist	Avail and/or Special
A	

SECONDARY ION MASS SPECTROMETRIC IMAGE DEPTH
PROFILE ANALYSIS OF THIN LAYERS

Paul K. Chu, William C. Harris, Jr., and George H. Morrison *

Baker Laboratory
Department of Chemistry
Cornell University
Ithaca, New York 14853

ABSTRACT: Image depth profiling is applied to the quantitative analysis of molecular beam epitaxially grown gallium arsenide thin layers. The technique involves the use of ion implantation through a mask and subsequent analysis by secondary ion mass spectrometry (SIMS). The proposed approach provides high accuracy results in the analysis of semiconductor thin layers.

* Author to whom reprint requests should be addressed.

Semiconductor materials research has succeeded in steadily reducing the physical size of electronic devices. With the development of epitaxial growth techniques, particularly molecular beam epitaxy (MBE) (1-3), layered structures of thicknesses on the order of 1 to 100 nm with precise composition profiles have been obtained. The fabrication of devices by MBE requires the ability to accurately add controlled quantities of electrically active dopants, a process which, in many cases, is not well understood. As experimentation continues, the need for accurate measurement of dopant concentration in such layers challenges the state-of-the-art of surface analytical techniques.

Secondary Ion Mass Spectrometry (SIMS) is currently recognized as one of the most sensitive techniques for the analysis of semiconductor materials (4,5), with detection limits in the ppm range for most elements. The application of ion implant standards (6-7) to SIMS has been developed to provide accurate quantitative concentration depth profiles. The method of solid state standard addition by ion implantation has been shown to give excellent results (8). This method involves implanting the sample with a controlled dose of the element to be determined, profiling through the implantation zone, and then comparing the integrated signal obtained from the implant to the background signal arising from the dopant being determined.

To insure complete removal of the implanted species, the residual dopant signal is acquired at a depth of at least three to four times that of the implant peak (8). This places a restriction on the minimum sample thickness which can be analyzed by this method. Furthermore, dopant inhomogeneity in the sample presents difficulties to the conventional

technique. Lateral (x-y) inhomogeneities can be dealt with only by the tedious process of running replicate analyses on several sampling areas. In-depth heterogeneity poses an even greater problem as all but gross inhomogeneities are masked within the implant region. Hence, effects such as diffusion towards the surface cannot be dealt with reliably. This problem can be circumvented in some instances by implanting with one isotope of the element of interest to serve as a standard and monitoring the residual component with another isotope. However, this is not always feasible as in the case of beryllium which is monoisotopic.

In order to reduce the thickness requirement to thinner layers, and to eliminate the problem of dopant inhomogeneity, the use of image depth profiling (9) was investigated. This technique fully utilizes the advantages of the ion microscope (10) by providing simultaneous in-depth analysis of several features within the ion image. Therefore, if the field of view of the image contains both implanted and unimplanted regions, implant and background signal levels can be obtained simultaneously to give quantitative concentration data. The only thickness limitation then becomes that necessary to contain the entire implant zone, while dopant heterogeneity can be visually assessed and determined quantitatively by proper choice of sampling areas within the ion image.

This method was applied to two thin layer samples. First, a quantitative determination of the beryllium dopant concentration in a 1 μm MBE grown gallium arsenide layer was performed as a test sample. The technique yielded a precision of 24% and was accurate to within 13%, both comparable to the results achieved by the conventional solid state

standard addition method. Next a GaAs layer containing a diffused silicon dopant was quantitatively analyzed.

EXPERIMENTAL SECTION

Instrumentation: The depth profiles were performed on a CAMECA IMS-3f ion microscope (11) interfaced with an HP 9845T computer for instrument control. A 400 nA O_2^+ primary beam at an energy of 5.5 keV relative to the sample was rastered over a $250\text{ }\mu\text{m} \times 250\text{ }\mu\text{m}$ area on the sample while the actual imaged field was $150\text{ }\mu\text{m}$ in diameter. Positive ions were monitored in all cases and all analyses were performed at the residual chamber vacuum of 3×10^{-8} torr. Depth measurements on the sputtered craters were performed on a Taylor Hobson TALYSTEP stylus profiler.

The Microscopic Image Digital Acquisition System (MIDAS) (12) was used to acquire the image depth profile data. MIDAS consists of a QUANTEX low light level ISIT TV camera, a GRINNELL digital frame buffer ($256 \times 240 \times 12\text{-bit}$ image), a DIGITAL BDP 11/34A minicomputer, and associated peripherals and software. The MIDAS system can acquire an image from the fluorescent screen of the ion microscope every 1/30th of a second or it can integrate images for an operator specified time for improved counting statistics. A further description can be found in Reference 12.

Computer Software: The image depth profile routines were written in FORTRAN and MACRO-11 while the implant peak integration program was written in FORTRAN. Programs to control the IMS-3f were written in BASIC for the HP 9845T computer. The image depth profile program allows the

operator to interactively select up to 30 rectangular sampling regions within the field of view ranging in size from one picture element (pixel) up to the entire image. The program sums a user defined number of frames, then computes the average pixel intensity within each sampling region, and converts to ion intensity using an empirically derived calibration equation. It records these intensities, then clears the frame buffer and begins to acquire a new image. The image depth profiling program has been previously described in detail (13).

Sample Preparation: The thin layer test sample used in this experiment was an 1 μm molecular beam epitaxially grown beryllium doped GaAs layer on a GaAs substrate. Prior to implantation, the residual beryllium dopant concentration was calculated using Hall effect measurements

to obtain the carrier concentration. For implantation, the sample was mounted onto an aluminum disc with conductive silver paint. A metal mask of 20 μm wide parallel slits spaced 150 μm apart was positioned over the sample which was then implanted with 2×10^{15} atoms/cm² ⁹Be at an energy of 60 keV, thus producing a series of implanted Be stripes.

The second sample analyzed was a 1 μm molecular beam epitaxially grown GaAs layer which had been doped with a uniform concentration of Si in the outer 200 nm during growth. The layer was then annealed at 400° C for 30 seconds under vacuum (10^{-8} torr). However it was suspected that the Si dopant had diffused into the bulk GaAs, either during growth or in the subsequent annealing step. This sample was implanted with 1×10^{15} atoms/cm² ²⁸Si at an energy of 200 keV using the same mask as the test sample.

RESULTS AND DISCUSSION

Figure 1 shows a schematic of the final implanted sample, while Figure 2 is the actual ion image of the implant acquired by the MIDAS system. The four $7\mu\text{m} \times 12\mu\text{m}$ sampling regions are also shown. Figure 3 is the image depth profile of regions 1 and 3. Regions 2 and 4 were used for the actual calculation, but were omitted here for clarity. As in the conventional solid state standard addition technique, the residual dopant concentration is calculated using equation 1.

$$C_r = \frac{S_r \times T \times F}{I \times D \times A} \quad (1)$$

In this equation, C_r is the residual dopant concentration to be determined in atoms/cm³, S_r is the residual dopant signal in cps, T is the total sputtering time in seconds, F is the fluence of the implant in atoms/cm², I is the integrated ion intensity of the implant peak in counts, D is the depth of the crater in centimeters, and A is the isotopic abundance of the dopant mass being monitored.

In order to gauge the capabilities of the image depth profile approach, the sample used in this experiment was deliberately chosen to be of sufficient thickness for analysis using the conventional solid state standard addition technique. The results obtained from these two methods, as well as the beryllium concentration as determined by Hall effect measurements,

are given in Table 1. The data for the SIMS measurements confirms that the image depth profiling technique is comparable to the conventional method in terms of accuracy and precision. Comparing the concentration values obtained shows the SIMS values to be higher than the

electrically measured value. While the discrepancy is within experimental error, it must be emphasized that the electrical measurement technique is only sensitive to beryllium which is electrically active. It is possible that some of the doped beryllium in the MBE GaAs layer has been incorporated into electrically inactive sites and is undetectable by electrical measurement.

As a further test of the image depth profiling approach, another GaAs MBE sample with the same Be dopant concentration was uniformly implanted to serve as an external calibration standard for the analysis of an unimplanted sample. The calculated Be concentration by this method yielded a 40% deviation from the electrical value, indicating the advantage of the image depth profiling technique over the external standard approach. This is due to the fact that the external standard method cannot take into account the instantaneous fluctuations of instrumental and analysis parameters. By analyzing the standard and unknown simultaneously, as in the image depth profiling technique, effects such as primary beam density, secondary ion transmission and chamber pressure variations are automatically eliminated.

The results of the beryllium doped test sample verify that this method is capable of giving accurate concentration values. To demonstrate its ability versus the conventional method, a sample with an in-depth inhomogeneity was chosen for quantitative analysis. Figure 4 shows the image depth profiles of the implanted stripe and unimplanted bulk. While the presence of the implanted species can be detected in the profile of the implanted region, it is difficult to accurately describe the actual diffusion profile beneath it. This is the limitation encountered using the conventional solid state

standard addition approach which uses a uniform implant of the entire sample surface. A sample such as this could not be readily analyzed by the conventional method. A deconvolution of the implant peak from a diffusion profile whose exact shape is not known is necessary.

The use of the image depth profiling technique, however, allows the operator to acquire both the implanted standard and a clear diffusion profile unobscured by the implant. Point by point subtraction of these two profiles directly gives the implant profile shown in Figure 5. This then can be used to quantify the diffusion profile through the application of equation 1 to generate an intensity to concentration conversion factor. In this case, it was found that

$$C = 1.9 \times 10^{16} \times n \quad (2)$$

where C is the elemental concentration in atoms/cm³, n is the secondary ion signal in counts/sec and the conversion factor has the unit atoms-secs/cm³ counts.

Using this factor, the signal intensities are readily converted to concentrations. The diffused silicon concentration is found to be 6.4×10^{20} atoms/cm³ at the surface, dropping to a constant residual level of 2.0×10^{17} atoms/cm³ at a depth of 320 nm. This example illustrates the ability of the image depth profiling approach to not only overcome sample heterogeneities, but to extract meaningful information with relative ease.

While the use of the image profiling technique eliminates errors caused by fluctuation of the analysis conditions, one effect that must be corrected for during data processing of the image depth profile is false image contrast caused by the imaging detector. The CAMECA IMS-3f ion microscope

uses a channel electron multiplier array (CEMA) (13), also known as a channelplate, as the ion to electron converter before the fluorescent viewing screen. In the course of normal usage, the original uniform ion intensity response across the channelplate surface begins to degrade. This results in a type of fixed pattern noise being present in all acquired images. Fortunately, the removal of this noise is straight forward. In this instance, images of ^{69}Ga from the GaAs sample, which would be expected to give a uniformly illuminated image, were used as reference images to determine the relative sensitivities of each pixel. These reference images were then used to correct all subsequent images for this nonuniformity. It should be noted that Figures 3,4 and 5 present data corrected for this effect, while the ion image of Figure 2 shows raw image data.

Although the image depth profiling technique gives excellent results for quantitative thin layer analysis, one requirement of any quantification methodology is that of sensitivity. Currently, the MIDAS system provides detection limits approximately two orders of magnitude higher than those obtained using conventional electron multiplier detection. This necessitated using a relatively high dopant concentration of 3×10^{19} atoms/cm³ as a test sample. However, the detection limits can be lowered significantly by judicious choice of the channelplate detector used. In particular, rather than using a single plate multiplier as is currently the case, a tandem dual plate arrangement would significantly boost the gain provided by the ion to electron conversion stage, thereby directly enhancing the systems sensitivity.

The advantages of the image depth profile approach to solid state standard addition are therefore threefold. By simultaneously analyzing the standard and the unknown, high accuracy is obtained. The successful analysis of layers three to four times thinner than can be done by the conventional solid state standard addition technique is possible since the image profiling method does not require complete removal of the implant zone before residual dopant signals are obtained. Instead, the minimum sample thickness is determined by the depth needed to contain the implant profile. Therefore, the use of low implantation energies to keep penetration depths to a minimum will allow the analysis of layers with thicknesses in the range of 50 to 500 nm depending on the atomic masses of the dopant and substrate.

Finally, since the entire ion image is monitored rather than being summed into one analysis point as in a standard depth profile, dopant heterogeneity within the sample does not present a problem to successful analysis. Lateral inhomogeneity is dealt with by positioning sampling areas over the various regions within the field of view suspected of being nonuniform. In addition, since only a small fraction of the sample contains the implanted standard, in depth heterogeneity occurring over the depth of the implant zone can be monitored and quantitatively analyzed in the unimplanted regions with much greater accuracy than would be provided by the use of external standards. Further improvements in the image detection system will allow increased sensitivity to provide quantitative concentration data for very low level dopants in thin layer semiconductor materials.

ACKNOWLEDGEMENT

The authors would like to acknowledge Susan Palmateer for preparing the MBE sample and doing the electrical measurements. Acknowledgement is also given to Harry Dietrich of the Naval Research Laboratory for the ion implantation.

CREDIT

Funding of this project was provided by the National Science Foundation, the Office of Naval Research, and the Cornell Materials Science Center.

LITERATURE CITED

- (1) Panish, M. B. Science 1980, 208, 916-922.
- (2) Cho, A. Y.; Arthur, J. R. "Progress in Solid State Chemistry", Somorjai, G.; McCaldin, J. Ed.; Pergamon, New York 1975, Vol. 10, 157-191.
- (3) Cho, A. Y. J. Vac. Sci. Technol. 1979, 16, 275-284.
- (4) Zinner, E. Scanning 1980, 3, 57-78.
- (5) McHugh, J. A. "Secondary Ion Mass Spectrometry" in "Methods of Surface-Analysis", Wolsky, S. P.; Czanderna, A. W. Ed., Elsevier, New York, 1976.
- (6) Gries, W. H. Int. J. of Mass Spec. and Ion Phys. 1979, 30, 97-112.
- (7) Gries, W. H. Mikrochim. Acta. 1981, 1, 335-342.
- (8) Leta, D. P.; Morrison, G. H. Anal. Chem. 1980, 52, 514-519.
- (9) Patkin, A. J.; Morrison, G. H. Anal. Chem. 1982, 54, 2-5.
- (10) Morrison, G. H.; Slodzian, G. Anal. Chem. 1975, 47, 932A-943A.
- (11) Ruberol, J. M.; Leqpareu, M.; Autier, B.; Gourgout, J.M. VIII Inter. Cong. on X-Ray Optics and Microanal. and 12th Ann. Conf. of the Micro-beam Analysis Society, Boston, Mass., 1977, 133A-133D.
- (12) Furman, B. K.; Morrison, G. H. Anal. Chem. 1980, 52, 2305-2310.
- (13) Woodhead, A. W.; Eschard, G. Acta Electronica 1971, 14, 181-200.

Table 1. The beryllium concentration as calculated from SIMS and electrical measurements. Standard deviations based on 10 replicate analyses.

	atoms/cm ³	std. dev.
Electrical	3.0×10^{19}	-
Image depth profile	3.4×10^{19}	0.6
Conventional SIMS	3.3×10^{19}	0.6

FIGURE CAPTIONS

- Figure 1. Implantation schematic
- Figure 2. MIDAS acquired Be image of the stripe implant. The rectangles show the four sampling areas
- Figure 3. Image depth profiles of region 1 (implanted) and region 3 (masked).
- Figure 4. Image depth profiles of unimplanted and implanted zones of ^{28}Si diffused into a GaAs MBE layer.
- Figure 5. The ^{28}Si implant profile obtained by subtracting the diffusion profile in the unimplanted region from the depth profile of the implanted region.

Figure 1

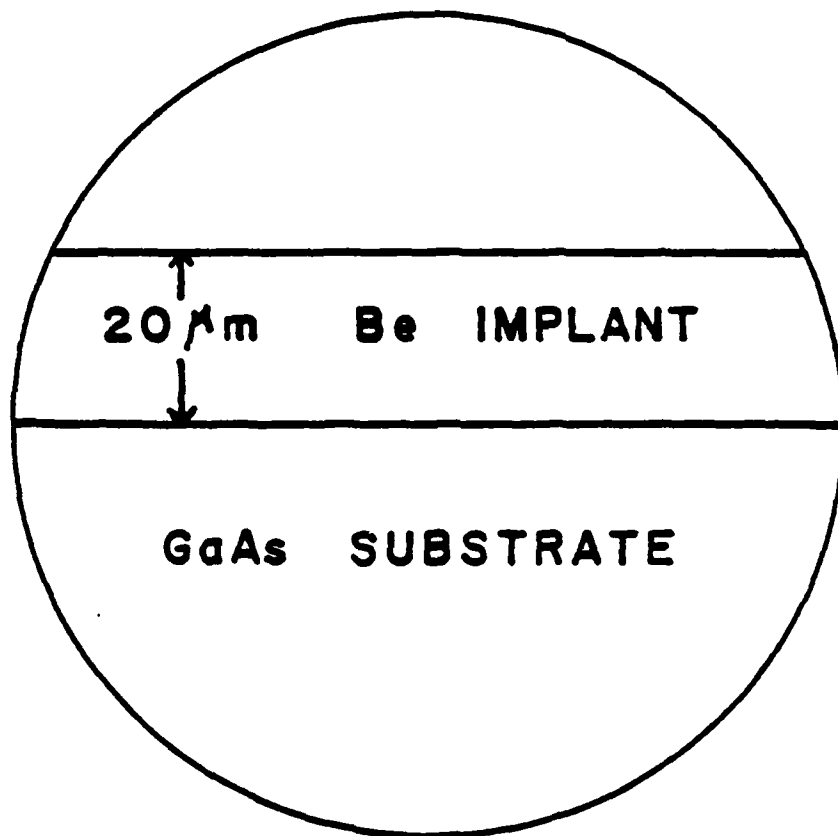


Figure 2

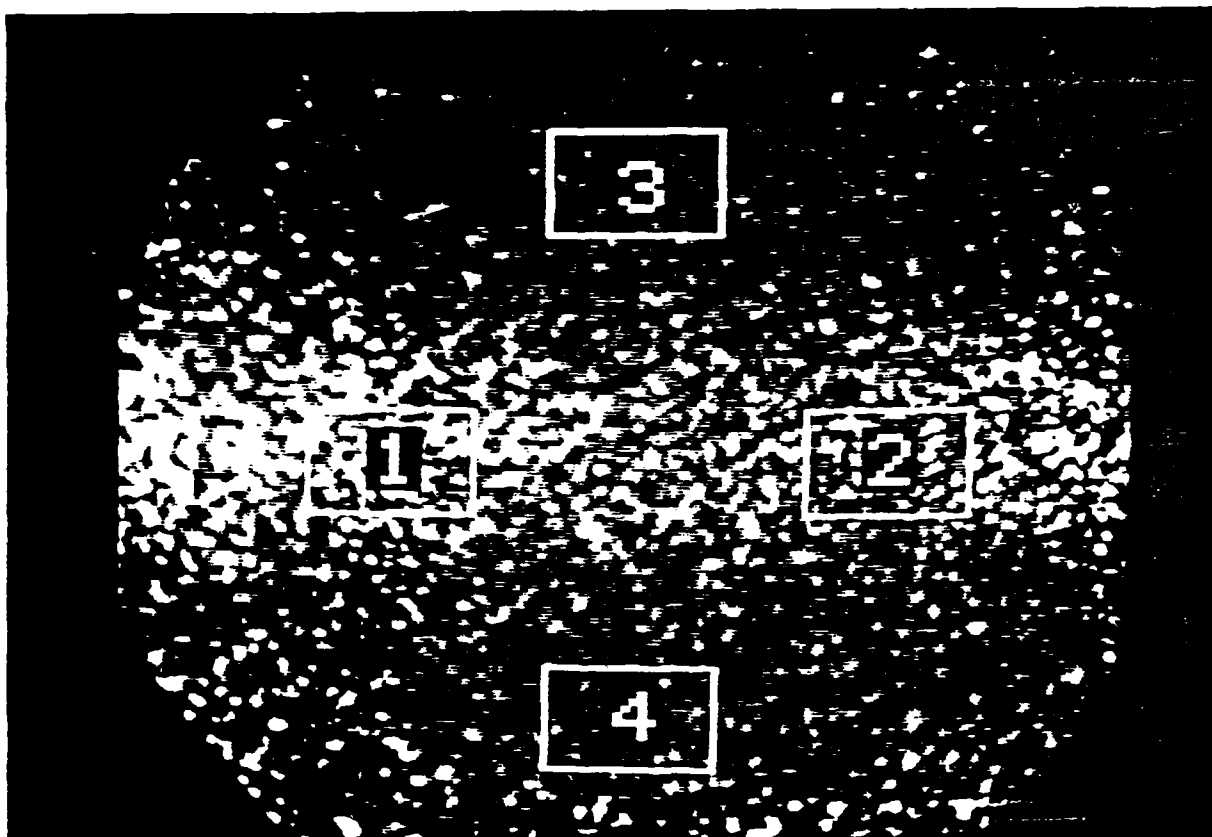


Figure 3

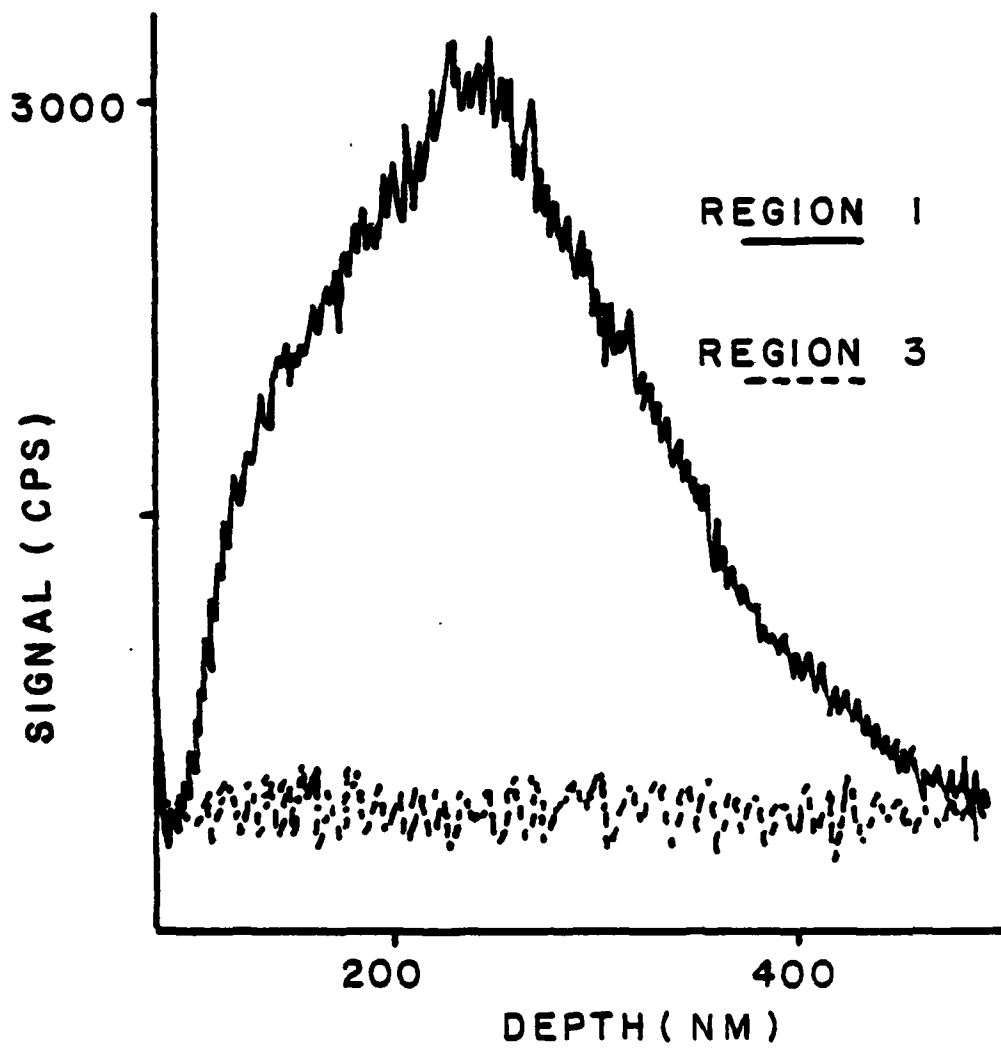


Figure 4

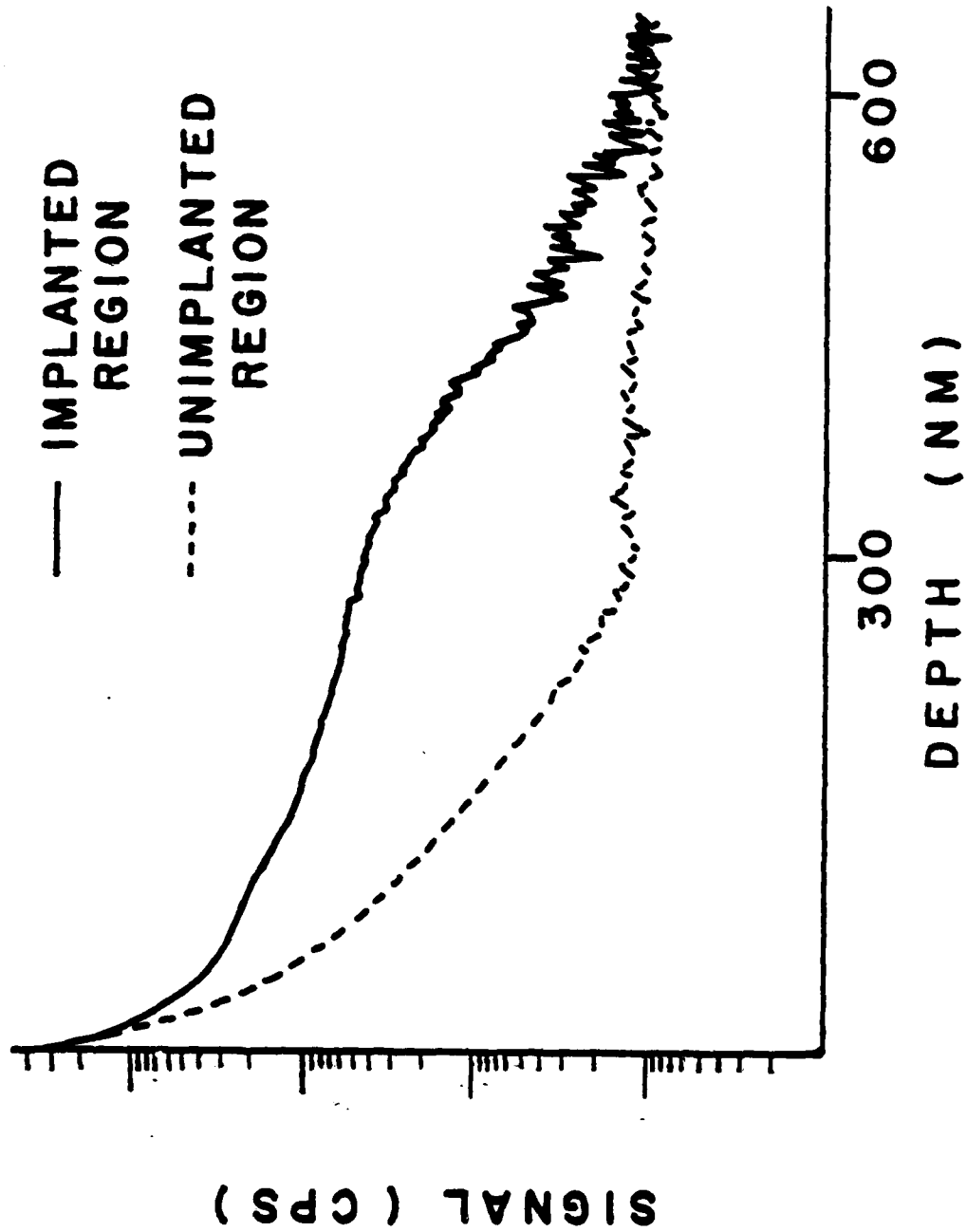
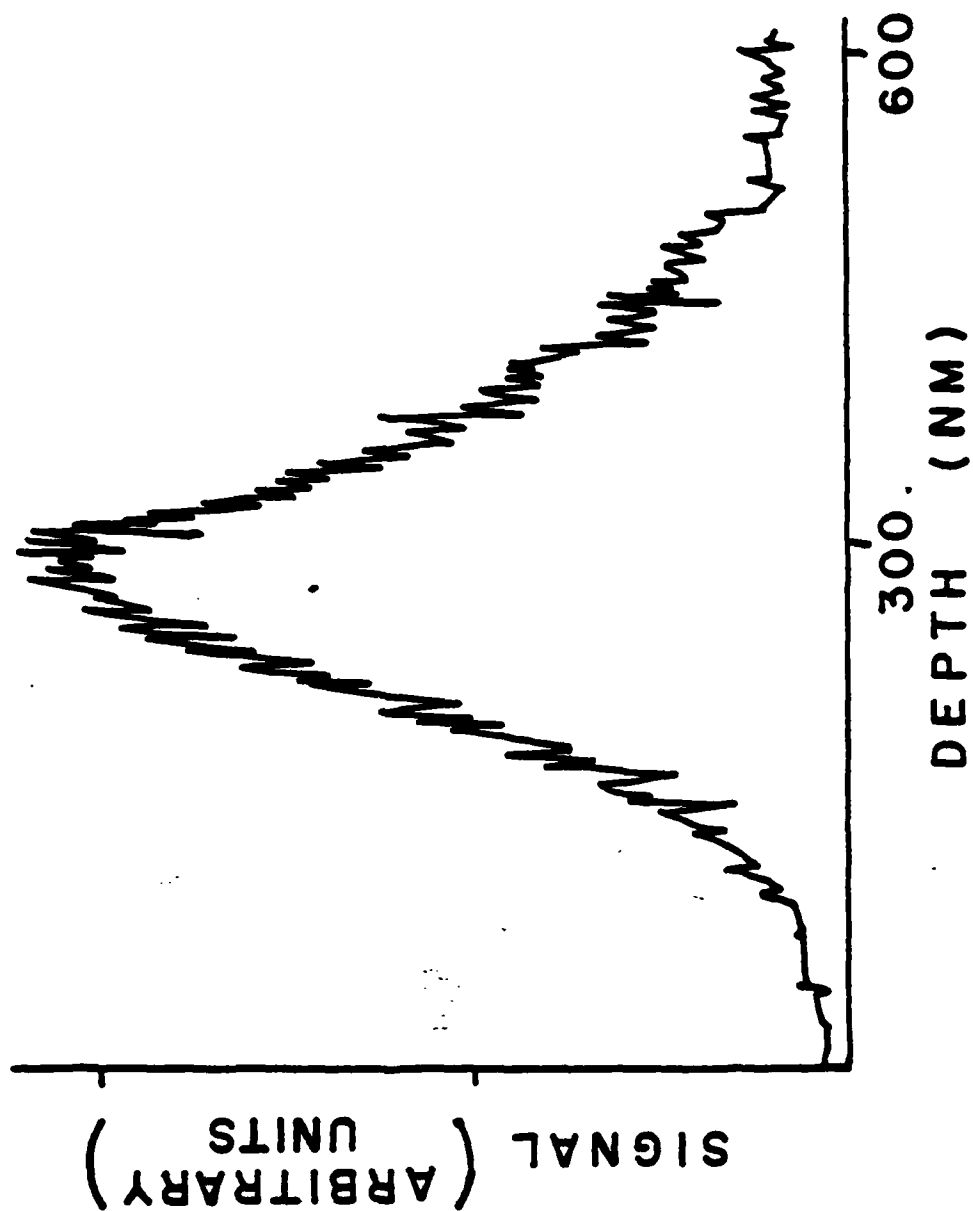


Figure 5



TECHNICAL REPORT DISTRIBUTION LIST, GEN

	<u>No. Copies</u>		<u>No. Copies</u>
Office of Naval Research Attn: Code 472 800 North Quincy Street Arlington, Virginia 22217	2	U.S. Army Research Office Attn: CRD-AA-IP P.O. Box 1211 Research Triangle Park, N.C. 27709	1
ONR Branch Office Attn: Dr. George Sandoz 536 S. Clark Street Chicago, Illinois 60605	1	Naval Ocean Systems Center Attn: Mr. Joe McCartney San Diego, California 92152	1
ONR Area Office Attn: Scientific Dept. 715 Broadway New York, New York 10003	1	Naval Weapons Center Attn: Dr. A. B. Amster, Chemistry Division China Lake, California 93555	1
ONR Western Regional Office 1030 East Green Street Pasadena, California 91106	1	Naval Civil Engineering Laboratory Attn: Dr. R. W. Drisko Port Hueneme, California 93401	1
ONR Eastern/Central Regional Office Attn: Dr. L. H. Peebles Building 114, Section D 666 Summer Street Boston, Massachusetts 02210	1	Department of Physics & Chemistry Naval Postgraduate School Monterey, California 93940	1
Director, Naval Research Laboratory Attn: Code 6100 Washington, D.C. 20390	1	Dr. A. L. Slafkosky Scientific Advisor Commandant of the Marine Corps (Code RD-1) Washington, D.C. 20380	1
The Assistant Secretary of the Navy (RE&S) Department of the Navy Room 4E736, Pentagon Washington, D.C. 20350	1	Office of Naval Research Attn: Dr. Richard S. Miller 800 N. Quincy Street Arlington, Virginia 22217	1
Commander, Naval Air Systems Command Attn: Code 310C (H. Rosenwasser) Department of the Navy Washington, D.C. 20360	1	Naval Ship Research and Development Center Attn: Dr. G. Bosmajian, Applied Chemistry Division Annapolis, Maryland 21401	1
Defense Technical Information Center Building 5, Cameron Station Alexandria, Virginia 22314	12	Naval Ocean Systems Center Attn: Dr. S. Yamamoto, Marine Sciences Division San Diego, California 91232	1
Dr. Fred Saalfeld Chemistry Division, Code 6100 Naval Research Laboratory Washington, D.C. 20375	1	Mr. John Boyle Materials Branch Naval Ship Engineering Center Philadelphia, Pennsylvania 19112	1
Dr. Rudolph J. Marcus Office of Naval Research Scientific Liaison Group - Amer. Embassy A.P.O. San Francisco, CA. 96503	1	Mr. James Kelley DTNSRDC Code 2803 Annapolis, Maryland 21402	1

TECHNICAL REPORT DISTRIBUTION LIST, 051C

	<u>No.</u> <u>Copies</u>		<u>No.</u> <u>Copies</u>
Dr. M. B. Denton Department of Chemistry University of Arizona Tucson, Arizona 85721	1	Dr. John Duffin United States Naval Postgraduate School Monterey, California 93940	1
Dr. R. A. Osteryoung Department of Chemistry State University of New York at Buffalo Buffalo, New York 14214	1	Dr. G. M. Hieftje Department of Chemistry Indiana University Bloomington, Indiana 47401	1
Dr. B. R. Kowalski Department of Chemistry University of Washington Seattle, Washington 98105	1	Dr. Victor L. Rehn Naval Weapons Center Code 3813 China Lake, California 93555	1
Dr. S. P. Perone Department of Chemistry Purdue University Lafayette, Indiana 47907	1	Dr. Christie G. Enke Michigan State University Department of Chemistry East Lansing, Michigan 48824	1
Dr. D. L. Venezky Naval Research Laboratory Code 6130 Washington, D.C. 20375	1	Dr. Kent Eisentraut, MBT Air Force Materials Laboratory Wright-Patterson AFB, Ohio 45433	1
Dr. H. Freiser Department of Chemistry University of Arizona Tucson, Arizona 85721	1	Walter G. Cox, Code 3632 Naval Underwater Systems Center Building 148 Newport, Rhode Island 02840	1
Dr. Fred Saalfeld Naval Research Laboratory Code 6110 Washington, D.C. 20375	1	Professor Isiah M. Warner Texas A&M University Department of Chemistry College Station, Texas 77840	1
Dr. H. Chernoff Department of Mathematics Massachusetts Institute of Technology Cambridge, Massachusetts 02139	1	Professor George H. Morrison Cornell University Department of Chemistry Ithaca, New York 14853	1
Dr. K. Wilson Department of Chemistry University of California, San Diego La Jolla, California	1	Professor J. Janata Department of Bioengineering University of Utah Salt Lake City, Utah 84112	1
Dr. A. Zirino Naval Undersea Center San Diego, California 92132	1	Dr. Carl Heller Naval Weapons Center China Lake, California 93555	1
		Dr. L. Jarvis Code 6100 Naval Research Laboratory Washington, D. C. 20375	1

DATE
FILMED
-8